

1 **THE MECHANISM OF ACID-BASE REGULATION IN**
2 **SEAWATER-ACCLIMATED GREEN CRABS, *CARCINUS***
3 ***MAENAS***

4
5 **S. Fehsenfeld^{1§}, D. Weihrauch¹**

6
7 ¹ Department of Biological Sciences, University of Manitoba, 190 Dysart Road,
8 Winnipeg, MB, Canada R3T2N2

9
10 Email addresses:

11 SF: Sandra.Fehsenfeld@umanitoba.ca

12 DW: Dirk.Weihrauch@umanitoba.ca

13
14 [§]Corresponding author:

15 Sandra Fehsenfeld

16 General Office 212B Bio-Sci Bldg., 50 Sifton Road

17 University of Manitoba, Winnipeg, MB R3T 2N2 Canada

18 Ph: 204-296 2106, Fax: 204-474-7604

19 Email: Sandra.Fehsenfeld@umanitoba.ca

20 **Abstract**

21 The present study investigated acid-base regulatory mechanisms in seawater-acclimated
22 green crabs *Carcinus maenas*. In seawater (32 ppt), this decapod crustacean is osmo-
23 conforming and therefore the majority of the observed responses can be attributed to ion
24 fluxes based on acid-base compensatory responses alone. Similar to what is observed in
25 brackish-water acclimated *C. maenas*, seawater-acclimated green crabs exposed to
26 environmental hypercapnia rapidly accumulated HCO_3^- in their hemolymph to compensate
27 for the respiratory acidosis caused by excess hemolymph $p\text{CO}_2$ after only 24-48 hours. A
28 full recovery of the decreased hemolymph pH was not observed in this time frame. Isolated
29 gill perfusion experiments on anterior gill 5 applying inhibitors for potential key-
30 transporters located in the crabs' gill epithelium supported the involvement of all
31 investigated genes in ammonia excretion and the excretion of acid-base equivalents. The
32 most significant effect was observed targeting basolateral applied $\text{Na}^+/\text{HCO}_3^-$ -
33 cotransporter and V-ATPase. Under the influence of these two inhibitors the excretion of
34 H^+ and partly for CO_2 was reversed and an enrichment of these two molecules in the
35 hemolymph was observed. A working model for acid-base regulatory mechanisms and
36 their link to ammonia excretion in the gill epithelium of *C. maenas* has been hypothesized
37 including basolateral $\text{Na}^+/\text{HCO}_3^-$ -cotransporter, V-ATPase, Na^+/H^+ -exchanger, Na^+/K^+ -
38 ATPase, carbonic anhydrase and K^+ -channels. The data of the present study suggests
39 transport of CO_2 and NH_4^+ in acidified and non-acidified vesicles.

40

41 Keywords: *Carcinus maenas*, green crab, CO_2 , ammonia, gill perfusion

42 **Introduction**

43 Over the last decades, green crabs (*Carcinus maenas*) have become one of the most
44 successful marine invaders on the planet (Lowe et al., 2000). Originating from northern
45 European waters, they nowadays can be found in both the Canadian Atlantic and Pacific,
46 where they threaten the existing natural ecosystem communities as well as commercial
47 fisheries (Cameron and Metaxas, 2005; Jamieson et al., 1998; Miron et al., 2005). The
48 success of *C. maenas* as an invasive species can be attributed to their high capability for
49 short-term acclimation as well as their potential for long-term adaptation to a variety of
50 environmental challenges such as changes in salinity, temperature, high ammonia and low
51 pO_2 / high pCO_2 (Bellwood, 2002; Thomsen et al., 2010; Truchot and Duhamel-Jouve,
52 1980; Weihrauch et al., 1999).

53 In decapod crustaceans like the green crab, this acclimation/adaptation potential is based
54 on the capability to maintain homeostasis of bodily fluids despite the changing
55 environment, which is mainly achieved *via* ion exchange processes in the gill epithelium.
56 Not only is the gill epithelium the major site for osmo-regulation, but it also plays an
57 important role in acid-base balance and ammonia excretion (Henry et al., 2012). While
58 over the past century extensive work has been conducted to investigate osmo-regulatory
59 and ammonia excretory patterns in gills of decapod crustaceans, hardly anything is known
60 concerning its acid-base regulation to date.

61 Resulting from tracer flux and voltage-clamp studies in Ussing chambers, the gill
62 epithelium of the green crab *Carcinus maenas* has been characterized as a (moderate) leaky
63 epithelium, exhibiting a relatively high trans-epithelial conductance and high ion transport
64 rates (Riestenpatt et al., 1996). Applying inhibitors in gill perfusion experiments and on

65 the split gill lamellae in similar experimental set-ups helped identify basolateral Na^+/K^+ -
66 ATPase and Cl^- -channels, as well as apical $\text{Na}^+/\text{K}^+/\text{2Cl}^-$ -cotransporter supported by apical
67 and basolateral K^+ -channels, to be the key-players in trans-branchial active NaCl transport
68 in moderate hyper-osmoregulators such as *C. maenas* and *Neohelice (Chasmagnathus)*
69 *granulatus* (Lucu and Siebers, 1987; Onken et al., 2003; Riestenpatt et al., 1996).
70 Basolateral Na^+/K^+ -ATPase and Cs^+ -sensitive K^+ -channels have also been shown to be
71 involved in ammonia excretion through the gills of *C. maenas*, as well as a cytoplasmic V-
72 ATPase and a functional microtubule network (Weihrauch et al., 1998, 2004). In
73 conclusion, these authors compared the NaCl uptake mechanism in the gill epithelium of
74 these decapod crustaceans to the mechanism also proposed for the thick ascending limb
75 (TAL) of the Henle's loop in the mammalian kidney. In addition to the transporters
76 mentioned above, the Na^+/H^+ -exchanger (NHE4) and the $\text{Na}^+/\text{HCO}_3^-$ -cotransporter
77 (NBCn1) have been identified in the basolateral membrane of the TAL to be involved in
78 ammonia re-absorption from the peritubular space into the epithelial cells (Houillier and
79 Bourgeois, 2012). In contrast to the mammalian TAL the current working model for acid-
80 base regulation of mitochondria-rich cells in the gills of freshwater teleosts supports a
81 basolateral, electrogenic $1\text{Na}^+/\text{3HCO}_3^-$ (NBC1) mediated base-excretion from the cell into
82 the blood, involving carbonic anhydrase and apical Na^+/H^+ -exchanger (isoforms 1 and 3;
83 Evans et al., 2005).
84 Unfortunately, to the authors' knowledge only one experiment on gill ion transporters in
85 respect to acid-base regulation has been conducted in decapod crustaceans to date. By
86 application of inhibitors and measuring the transepithelial potential difference (PDte) in
87 perfusion experiments on the isolated gill in brackish-water acclimated green crabs, Siebers

et al. (1994) identified oxidative metabolism and carbonic anhydrase to play the central roles in acid-base regulation by the gill epithelium. On the other hand the authors excluded active proton excretion, apical Na^+/H^+ -exchange, anion exchange, or $\text{Na}^+/\text{K}^+/\text{2Cl}^-$ -cotransport to participate in acid-base regulation of the gill epithelium.

On the whole animal level however, a direct link between acid-base regulation and ammonia status to salinity acclimation in decapod crustaceans has been delivered by a few studies. When acclimated to dilute salinities, blue crabs *Callinectes sapidus* elevated hemolymph ammonia levels, while at the same time hemolymph pH and HCO_3^- increased at constant $p\text{CO}_2$ (Mangum et al, 1976). A similar response was observed in *Carcinus maenas* (J. P. Truchot, 1981) and the Chinese mitten crab *Eriocheir sinensis* (Henry and Cameron, 1982). Additionally, acid-base status in crabs is dependent on the strong ion difference: the adjustments in hemolymph Na^+ and Cl^- concentrations due to dilute salinity acclimation are balanced by the weaker ions H^+ , OH^- and HCO_3^- in order to maintain the electrical neutrality of the body fluids (Stewart, 1978). In a third study, inhibition of CA, a major key-player in acid-base balance by promoting the dissociation of H_2CO_3 (CO_2) into H^+ and HCO_3^- , simultaneously led to a dose-dependent decrease in hemolymph osmolarity and Na^+ and Cl^- concentrations in low salinity acclimated *Pachygrapsus crassipes* (Burnett et al., 1981), *C. sapidus* (Henry and Cameron, 1983) and *C. maenas* (Henry et al., 2003).

Based on these links of ammonia and acid-base regulation on the organismal level in decapod crustaceans, it can be hypothesized that also on the level of the gill epithelium transporters known to be involved in salinity acclimation will play an important role in acid-base regulation in decapod crustaceans.

110 While most studies on osmo-regulation in decapod crustaceans have been conducted in
111 brackish-water acclimated specimen, the present study concentrates on seawater-
112 acclimated green crabs. At 32 ppt, *C. maenas* is osmo-conforming and keeps its
113 hemolymph osmolality isotonic to the surrounding seawater. As a result, NaCl movements
114 are believed to be mainly passive (Zanders, 1980), as also supported by the high
115 transepithelial conductance measured in gills of the marine osmoconforming edible crab
116 *Cancer pagurus* (Weihrauch et al., 1999). This allows for the investigation of the most
117 basic underlying principles of acid-base regulation in these osmo-conforming animals,
118 uncoupled from a salinity-mediated response. In a first set of experiments, acid-base
119 homeostasis in the seawater-acclimated green crabs was challenged by exposure to high
120 environmental $p\text{CO}_2$ (hypercapnia) in order to observe the whole animal response and the
121 capability of osmo-conforming green crabs to counteract this disturbance without an
122 already activated ion regulatory mechanisms being in place. In a second approach,
123 pharmaceuticals for the inhibition of distinct transporters potentially involved in acid-base
124 regulation were applied in isolated gill perfusion experiments of seawater-acclimated *C.*
125 *maenas* to identify key-players participating in this process. Based on these results, a novel
126 working model for acid-base regulatory mechanisms and their link to ammonia excretion
127 is postulated for the gill epithelium of seawater-acclimated green crabs.
128

129 **Material & Methods**

130 **Animals**

131 Green crabs *Carcinus maenas* (Linnaeus 1758) were collected in Barkley Sound at the
132 opening of the Pipestem Inlet (Vancouver Island, BC, Canada) in the Summer 2012 and
133 2013 under the Department of Fisheries and Oceans collection permits XR 207 2012 and
134 XR 235 2013, respectively. Only male animals with an approximate carapace width of 5-7
135 cm and a weight of 60 – 90 g were chosen for experimentation. Green crabs were kept in
136 aerated ~500 L flow-through outdoor tanks directly connected to water from the Barkley
137 Sound (salinity = 32 ppt) under natural light conditions (10(dark):14(light)) at the Bamfield
138 Marine Sciences Centre (Bamfield, BC, Canada). Animals were fed *ad libitum* once a week
139 with fish carcasses and starved for 2-3 days prior to experimentation.

140

141 **Acclimation to high environmental $p\text{CO}_2$ (hypercapnia)**

142 For acclimation to hypercapnic conditions (1% CO_2 = 1013.25 Pa), two aerated flow-
143 through plastic containers (68 L) were set up in the laboratory space and 6 green crabs
144 transferred into each. A header tank for each container was established, supplying
145 containers with either fresh seawater (controls) or seawater pre-equilibrated to 1% CO_2
146 (high $p\text{CO}_2$). The flow rate from the header tanks to the containers holding the animals was
147 adjusted to 50 ml / min.

148 To easily draw hemolymph from the animals a hole (diameter ~2mm) was drilled into the
149 dorsal carapace using a Dremel® and sealed with dental dam. A sterile syringe with a 21.5
150 gauge needle was used to obtain ~200 μl hemolymph samples at 0, 6, 12, 24, and 48 hours,

151 respectively. Hemolymph was immediately assessed for pH and total carbon (C_T) as
152 described below. Samples were then frozen at -20°C until analyzed for ammonia content
153 (see below).

154 To determine whole animal ammonia excretion rates, green crabs were transferred into
155 small aerated containers holding 2 L of seawater, after being acclimated to either control
156 or high $p\text{CO}_2$ seawater in the 68 L tanks for 48 h, as described above. 10 ml water samples
157 were taken after 10 and 40 minutes and frozen at -20°C until further analysis for ammonia
158 (see below).

159

160 **Gill perfusion with application of inhibitors**

161 Isolated anterior gills (gill 5) of control seawater-acclimated animals were perfused
162 following the protocol of Siebers et al. (1985) with a flow rate of $128 \pm 0.1 \mu\text{L}/\text{min}$, using
163 a peristaltic pump (Sci 323 Watson–Marlow Bredel Pump, Falmouth Cornwall, England).
164 Gills were placed in 50 ml glass beakers containing 30 ml seawater as bathing solution.
165 The perfusion solution contained (in mmol L^{-1}): 470 NaCl, 12 CaCl_2 , 12 MgCl_2 , 11 KCl, 9
166 NaHCO_3 , 0.3 Glucose, 0.1 Glutathion, 0.5 Glutamine, based on results from ion
167 chromatography performed on hemolymph of full strength seawater-acclimated green
168 crabs in context of the recent study by Fehsenfeld and Weihrauch (2013; data not shown).
169 The pH was adjusted to 7.9. $100 \mu\text{mol L}^{-1} \text{NH}_4\text{Cl}$ was solely added to the perfusion
170 solution, not the bathing solution, to account for *in vivo* conditions.

171 The perfusion protocol consisted of 3 consecutive steps (figure 1): following a 40 min
172 control phase, gills were perfused with perfusion solution containing the respective
173 inhibitor (see below). A third 40 minute period applying perfusion solution as in the control

174 step (step 1) was implemented to ensure that the gills were still active (returning to control
175 levels). In between each step, the gills were allowed a 10 minute equilibration period after
176 which the perfusate was collected then for 30 min.

177 The inhibitors and their concentrations were 100 $\mu\text{mol L}^{-1}$ tenidap ($\text{Na}^+/\text{HCO}_3^-$ -
178 cotransporter, NBC), 20 $\mu\text{mol L}^{-1}$ KM91104 (V-ATPase), 5 mmol L^{-1} ouabain (Na^+/K^+ -
179 ATPase, NKA), 100 $\mu\text{mol L}^{-1}$ amiloride (Na^+/H^+ -exchanger, NHE) and 12 mmol L^{-1} BaCl_2
180 (K^+ -channels). All inhibitors with the exception of ouabain were diluted from 100x
181 concentrated stock solutions in DMSO. Ouabain was directly dissolved in the perfusion
182 solution. Perfusion experiments with 1% DMSO alone in the inhibitor step were performed
183 and found to neither have an affect ammonia excretion, nor acid-base equivalents ($n = 3$,
184 data not shown).

185

186 **Analysis of hemolymph and perfusate samples**

187 All hemolymph and perfusate samples were immediately measured for the acid-base
188 equivalents pH and C_T (and temperature). pH was measured either with the InLab Micro
189 Combination pH electrode (hemolymph – small volumes; Mettler-Toledo) or the pH/ATC
190 electrode #300729.1 (perfusates – big volumes; Denver Instruments, Göttingen, Germany),
191 connected to a pH-ISE meter model 225 (Denver Instruments). Total CO_2 (C_T) was
192 measured using the Corning 965 carbon dioxide analyzer (Olympic Analytical Service,
193 UK). $p\text{CO}_2$ and HCO_3^- were then calculated applying the appropriate factors and equations
194 as generated by Truchot (1976).

195 Hemolymph ammonia, perfusate ammonia and ammonia contents of the seawater samples
196 from the whole animal excretion experiment were measured using a gas-sensitive NH_3

197 electrode (Orion 9512 from Thermo Scientific, Cambridgeshire, England) connected to a
198 digital mV/pH meter, following the procedure established by Weihrauch et al. (1998). All
199 samples were diluted as high salt has been found to interact with the electrode (1:3 in case
200 of the perfusates / water samples, 1:7 in case of hemolymph samples due to low volumes).
201 Standard curves were diluted accordingly.

202 Gill excretion rates for ammonia and acid-base equivalents were assessed based on the
203 difference of the respective concentration in the perfusate compared to the initial perfusion
204 solution for each step. H^+ excretion was calculated from the change in perfusate pH vs. the
205 initial pH of the perfusion solution of each step, respectively.

206

207 **Statistics**

208 All statistical analyses were performed using the software Past3 (Hammer et al., 2001). All
209 data sets were first tested for normal distribution (Shapiro–Wilk test) and homogeneity of
210 variances (F-test or Levene’s test) prior to testing. In case normal distribution and/or
211 homogeneity of variances were not fulfilled, the data sets were log-transformed or tested
212 with non-parametric tests. Concerning parametric testing, Student’s t-test or paired t-test
213 was applied comparing two means, whereas one-way ANOVA was applied comparing
214 multiple data sets. In case of non-parametrical testing, Mann-Whitney U-test was applied
215 for comparison of two means, and Kruskal-Wallis accordingly for multiple means. All
216 results with $p < 0.05$ were considered significant.

217 **Results**

218 **Whole organism response of *C. maenas* upon high $p\text{CO}_2$ exposure**

219 Green crabs rapidly accumulated CO_2 and HCO_3^- in their hemolymph as response to high
220 $p\text{CO}_2$ exposure (1% CO_2) as can be seen in figure 2. A significant increase in both
221 hemolymph parameters was observed after only 6 hours and equilibrated at a 4-fold
222 increased level for $p\text{CO}_2$ (688 ± 40 Pa), and a 3-fold increased level for HCO_3^- (19 ± 2
223 mmol L^{-1}) after 48 hours exposure, respectively. Interestingly, the increase in HCO_3^- did
224 not seem to be sufficient to completely counteract / buffer the respiratory acidosis and pH
225 values decreased by 1.1 units from control values of 7.87 ± 0.02 to 7.76 ± 0.03 in high
226 $p\text{CO}_2$ crabs after 48 hours.

227 Hemolymph ammonia increased significantly from $93 \pm 0.8 \mu\text{mol L}^{-1}$ in control animals to
228 $406 \pm 45 \mu\text{mol L}^{-1}$ in high $p\text{CO}_2$ crabs, as did the whole animal ammonia excretion rates
229 (46 ± 10 versus $175 \pm 34 \text{ nmol g}^{-1} \text{ h}^{-1}$).

230

231 **Effects of inhibitors in gill perfusion experiments of seawater-acclimated green crabs**

232 Under control conditions, gill 5 excreted all of the investigated parameters ammonia, H^+
233 and CO_2 (lower concentration in perfusate compared to the initial perfusion solution, figure
234 3). Compared to green crabs acclimated to brackish-water (10 ppt, data from Fehsenfeld
235 and Weihrauch (2013)), *C. maenas* acclimated to full-strength seawater (32 ppt, present
236 study) generally excreted less H^+ and CO_2 , while excretion rates for ammonia and HCO_3^-
237 were the same as for brackish-water acclimated animals.

238 The by far most drastic effects of inhibitors were observed with basolateral application of
239 tenidap ($\text{Na}^+/\text{HCO}_3^-$ -cotransporter) and KM91104 (V-ATPase) on H^+ and CO_2 excretion
240 rates by isolated gill 5, respectively (figure 4). Blocking a potential basolateral situated
241 $\text{Na}^+/\text{HCO}_3^-$ -cotransporter resulted in an accumulation of protons (figure 4A) and CO_2
242 (figure 4B) in the hemolymph. Inhibiting V-ATPase basolaterally on the other hand only
243 led to the accumulation of protons in the hemolymph (figure 4A) and additionally, resulted
244 in a significantly decreased CO_2 excretion (*ca.* 70%, figure 4B) over the gill epithelium.
245 The $\text{Na}^+/\text{HCO}_3^-$ -cotransporter seemed not to be involved in ammonia excretion in posterior
246 gill 5 (figure 4C). While the apical application of tenidap ($\text{Na}^+/\text{HCO}_3^-$ -cotransporter) did
247 not affect any of the parameters H^+ , CO_2 and ammonia excretion, apical KM91104 (V-
248 ATPase) resulted in a significant decrease of H^+ (figure 4A) and CO_2 excretion (figure
249 4.B).

250 Also all of the other basolaterally applied inhibitors significantly decreased H^+ excretion
251 over the gill epithelium (figure 4A). While the decrease accounted for only 20% regarding
252 Na^+/K^+ -ATPase, blocking K^+ -channels, Na^+/H^+ exchanger and carbonic anhydrase resulted
253 in app. 50-60% less excretion of H^+ .

254 With the exception of the Na^+/H^+ -exchanger, all investigated transporters contributed
255 significantly to the excretion of CO_2 (figure 4B). Again, inhibition of the Na^+/K^+ -ATPase
256 led to the lowest reduction of *ca.* 20%, while blocking K^+ -channels and carbonic anhydrase
257 resulted in a decrease of CO_2 excretion by *ca.* 50%.

258 Besides basolateral V-ATPase as mentioned before, blocking Na^+/K^+ -ATPase, K^+ -
259 channels and Na^+/H^+ exchanger significantly reduced ammonia excretion over the gill
260 epithelia to a similar extend of *ca.* 50% (figure 4C).

261

262 **Discussion**

263 **Systemic response of seawater-acclimated *Carcinus maenas* upon disturbance of acid-** 264 **base homoeostasis**

265 Seawater-acclimated green crabs *Carcinus maenas* exhibited a rapid respiratory acidosis
266 in response to elevated environmental $p\text{CO}_2$ (48h, 1% $\text{CO}_2 = 1 \text{ kPa} = 7.5 \text{ mmHg}$). The
267 initial increase of $p\text{CO}_2$ from 264 ± 45 to $460 \pm 43 \text{ Pa}$ after 6 hours leveled off after 48
268 hours at 3-fold increased levels to stay just below environmental levels, while at this point
269 HCO_3^- is elevated by 2-fold. These general changes in acid-base status and the observed 4-
270 fold increase in hemolymph ammonia as well as ammonia excretion rates (2.5-fold) after
271 48 hours were similar to what has been observed in two recent studies on brackish-water
272 acclimated green crabs (0.4% $\text{CO}_2 = 0.4 \text{ kPa} = 3 \text{ mmHg}$; Appelhans et al., 2012 (10 weeks
273 exposure); Fehsenfeld and Weihrauch, 2013 (7 days exposure)) and the marine Dungeness
274 crab, *Metacarcinus magister* (Hans et al., 2014 (7-10 days exposure)).

275 Surprisingly however, the 2-fold increase in hemolymph HCO_3^- levels as observed in the
276 current study seemed not to be able to fully compensate the pH drop resulting from the
277 elevated hemolymph $p\text{CO}_2$. Consequently, hemolymph pH drops 0.11 units from $7.87 \pm$
278 0.01 to 7.76 ± 0.02 . Similarly, also freshwater blue crabs *Callinectes sapidus* were not able
279 to fully restore blood pH in this time frame as response to 1% CO_2 exposure (Cameron,
280 1978). In contrast, brackish-water acclimated green crabs restored their hemolymph pH
281 completely after 7 days, however no data is available for the initial phase of hypercapnia-
282 acclimation (Fehsenfeld and Weihrauch, 2013). While a comparable increase in blood

283 $p\text{CO}_2$ and HCO_3^- was observed in several seawater-acclimated fish as response upon
284 acclimation to 1% CO_2 (Brauner and Baker, 2009), their capability of restoring blood pH
285 varied strongly (Hayashi et al., 2004). After a drop of blood pH by 0.1-0.3 units pH
286 returned to control levels after only 1-3 hours in the yellowtail *Seriola quinqueradiata* and
287 the Japanese flounder *Paralichthys olivaceus*. In contrast, blood pH in starspotted dogfish
288 *Mustelus manazo* needed 72 hours to recover to control levels (Hayashi et al., 2004). An
289 uncompensated drop in pH as seen in this study was also observed in brackish-water
290 acclimated green crabs exposed to 14 days of high environmental ammonia (1 mmol L⁻¹
291 NH_4Cl ; Fehsenfeld et al., 2015; chapter 3). In this case the authors argued that, while this
292 level of pH decrease might not yet be harmful to the organism, it might rather be helpful
293 to increase $[\text{NH}_4^+]$ in the blood while reducing the amount of NH_3 , allowing for a tighter
294 control of ammonia levels *via* active transport by the Na^+/K^+ -ATPase (Weihrauch et al.,
295 1998). Unfortunately in the present study, changes in hemolymph acid-base parameters
296 could only be observed for 48 hours due to time constraints. Further experimentation needs
297 to be done in order to identify a time point for a potential complete restoration of
298 hemolymph pH.

299 Hemolymph ammonia levels in seawater-acclimated control green crabs were initially
300 lower than in brackish-water acclimated control animals, but then rose twice as high in
301 seawater + hypercapnia-acclimated animals compared to brackish-water + hypercapnia-
302 acclimated crabs (this study; Fehsenfeld and Weihrauch, 2013). These generally lower
303 ammonia contents are likely due to the fact that seawater-acclimated green crabs are not
304 osmo-regulating and therefore exhibiting a lower metabolic rate in contrast to the hyper-
305 regulating brackish-water acclimated animals, a phenomenon that has been observed in

306 other marine crustaceans like the prawn *Metapenaeus monoceros* (Rao, 1958). The
307 increase in hemolymph ammonia in seawater-acclimated green crabs as response to the
308 acid-base disturbance then might be explained by an increase in the resting metabolic rate
309 to counteract the respiratory acidosis, a response also observed in the blue mussel *Mytilus*
310 *edulis* (Thomsen and Melzner, 2010). This potential increase in metabolic rate in seawater
311 + hypercapnia-acclimated green crabs stands in contrast to the response of Dungeness crabs
312 acclimated to high $p\text{CO}_2$ that clearly exhibit a metabolic depression correlated with
313 decreased hemolymph ammonia and whole animal ammonia excretion rates (Hans et al.,
314 2014).

315 Interestingly, ammonia excretion rates in both seawater and brackish-water acclimated
316 *C. maenas* increased to the same extend (2.5-fold), independent on the initial hemolymph
317 ammonia concentration (this study; Fehsenfeld and Weihrauch, 2013). This indicates that
318 in response to hypercapnia, hemolymph ammonia levels are regulated to a very distinct
319 level beneficial for the organism, according to its physiological state (i.e. osmo-conforming
320 vs. hyper-regulating). While in seawater + hypercapnia-acclimated green crabs hemolymph
321 ammonia seems to become increasingly important as a buffer for acid-base balance, the
322 activated ion-regulatory machinery in the hyper-regulating *C. maenas* might already
323 provide an efficient transporter inventory for counteracting the acid-base disturbance,
324 decreasing the involvement of hemolymph ammonia.

325

326 **Excretory patterns of isolated gills of seawater and brackish-water acclimated *C.***
327 ***maenas***

328 Interestingly, when acclimated to brackish-water, gill epithelia from anterior gills are more
329 efficient in excreting protons and CO₂ than anterior gill epithelia of osmo-conforming
330 green crabs (figure 3B, C). This supports the hypothesis that anterior gills in general are
331 mainly involved in gas (CO₂) exchange processes as suggested by Compere et al., (1989)
332 and Freire et al. (2008). Additionally in contrast to posterior gills, anterior gills do not
333 undergo major structural changes due to acclimation to dilute salinity (Compere et al.,
334 1989). This indicates that the adjustment of acid-base regulatory mechanisms in anterior
335 gills are likely based on changes in gene expression levels of already present transporters
336 or their activity, rather than being “re-invented” as observed in posterior gills.

337 Interestingly, ammonia excretion rates of anterior gill 5 seemed to be independent of
338 environmental salinity, supporting findings of a recent study by Fehsenfeld et al. (2015).
339 This is surprising because whole animal excretion rates were observed to be significantly
340 (3-fold) higher in osmo- conforming green crabs compared to osmo-regulating green crabs.
341 As also discussed in the previous study by Fehsenfeld et al. (2015), this might indicate an
342 increased role for alternative ammonia-excretory structures like the antennal glands in
343 osmo-conforming crabs. Expression of the Rhesus-like protein, known to be involved in
344 ammonia excretion in the osmo-conforming Dungeness crabs for example significantly
345 increased in antennal glands but not in the gills when animals were exposed to high
346 environmental ammonia (Martin et al., 2011). Further research needs to be done to verify
347 the role of antennal glands in ammonia regulation in *C. maenas*.

348

349 **Identified transporters to be involved in acid-base and ammonia regulatory capacities**
350 **of isolated anterior and posterior gills**

351 With the exception of tenidap ($\text{Na}^+/\text{HCO}_3^-$ -cotransporter), all inhibitors tested in this study
352 were observed to clearly affect the excretion rates for both, ammonia and acid-base
353 equivalents, therefore strengthening the hypothesis that both processes are linked in the gill
354 epithelium of *Carcinus maenas*.

355 To the authors knowledge this is the first study to identify **basolateral $\text{Na}^+/\text{HCO}_3^-$ -**
356 **cotransporter** to be a key-player for acid-base regulation in *C. maenas*. In a recent study
357 on low salinity acclimation however, the $\text{Na}^+/\text{HCO}_3^-$ -cotransporter was up-regulated 1.3-
358 fold in posterior gills of brackish-water acclimated *C. maenas* in comparison to seawater-
359 acclimated green crabs (Towle et al., 2011), and seems generally to be higher expressed in
360 posterior gills of these animals (Fehsenfeld and Weihrauch, 2013). Interestingly however,
361 this transcript was not affected in brackish-water acclimated *C. maenas* by acclimation to
362 hypercapnia (Fehsenfeld et al., 2011). A basolateral $\text{Na}^+/\text{HCO}_3^-$ -cotransporter has also been
363 postulated to be involved in acid-base regulation in the osmo-conforming crab *Neohelice*
364 (*Chasmagnathus*) *granulata* (Tresguerres et al., 2008) and recently, a basolateral
365 $\text{Na}^+/\text{HCO}_3^-$ -cotransporter has been identified to be of high importance in acid-base
366 regulation in the squid *Sepioteuthis lessoniana* (Hu et al., 2014). Also in the thick ascending
367 loop of Henle in the mammalian kidney (TAL), a basolateral $\text{Na}^+/\text{HCO}_3^-$ -cotransporter has
368 been observed, transporting HCO_3^- and Na^+ from the blood into the cell (Krapf, 1988).
369 When the $\text{Na}^+/\text{HCO}_3^-$ -cotransporter from rat kidney is expressed in *Xenopus laevis*
370 oocytes, the transporter could be inhibited by the inflammatory drug tenidap (Madhok,
371 1995) and has been shown to work with different stoichiometric ratios (2:1 and 3:1 HCO_3^-

372 :Na⁺; Ducoudret et al., 2001). Due to the similarity of the transporter inventory (apical
373 Na⁺/K⁺/2Cl⁻ cotransporter, basolateral Na⁺/K⁺-ATPase, K⁺-and Cl⁻-channels), Riestenpatt
374 et al. (1995, 1996) compared the gill epithelium of *C. maenas* with the mammalian TAL,
375 therefore a similar distribution and function of the Na⁺/HCO₃⁻-cotransporter can be
376 postulated. A basolateral Na⁺/HCO₃⁻-cotransporter as suggested in the present study would
377 provide the major carbonic anhydrase-independent HCO₃⁻ source for the epithelial cell. In
378 contrast, data of this study does not indicate an apical component of this transporter.

379 **V-ATPase** on the other hand had been observed to be involved in active ammonia excretion
380 in brackish-water acclimated green crabs (Weihrauch et al., 2002). In contrast to
381 freshwater-acclimated crustaceans like the Chinese mitten crab *Eriocheir sinensis*, the
382 investigated B subunit of V-ATPase in *C. maenas* is not involved in osmoregulation and
383 therefore not essential for the electrochemical gradient of epithelial cells (Weihrauch et al.,
384 2001). While expression of V-ATPase in the freshwater-acclimated *E. sinensis* (Onken and
385 Putzenlechner, 1995) and the freshwater crab *Dilocarcinus pagei* (Weihrauch et al., 2004)
386 is higher in posterior gills, it tends to be more abundant in anterior gills of *C. maenas*
387 (Fehsenfeld and Weihrauch, 2013; Weihrauch et al., 2001). Due to the mainly cytoplasmic
388 distribution of V-ATPase in gill epithelial cells of brackish-water acclimated green crabs,
389 the authors rather postulated its presence in the membrane of vesicles that are acidified by
390 V-ATPase in order to trap ammonia for exocytosis, being transported along the
391 microtubule network (Fehsenfeld et al. 2015; Weihrauch et al., 2001). This hypothesis is
392 supported by the results of the present study as ammonia as well as H⁺ and CO₂ excretion
393 is inhibited by the V-ATPase blocker KM91104 (Kartner et al., 2010). A primarily apical
394 distribution as seen in many freshwater fish seems unlikely for seawater and brackish-water

395 acclimated crustaceans (Gilmour and Perry, 2009; Weihrauch et al., 2001). Interestingly
396 however, an effect of apically applied KM91104 was observed for H^+ and CO_2 excretion
397 and may be attributed to the presence of V-ATPase in the apical membrane due to the
398 fusion of the V-ATPase carrying vesicles.

399 As suggested by the present data, basolateral **Na^+/K^+ -ATPase and K^+ -channels** are
400 essential not only for the excretion of ammonia, but also all acid-base equivalents. This is
401 not surprising as both transporters have been shown to directly promote NH_4^+ (and
402 therefore H^+) entry from the hemolymph into gill epithelial cells by NH_4^+ substituting for
403 K^+ (Lignon, 1987; Skou, 1960; Weihrauch et al., 1998). Also in elasmobranchs, Na^+/K^+ -
404 ATPase plays an important role in acid-base balance (Gilmour and Perry, 2009). By
405 generating an electrochemical gradient over the basolateral membrane by pumping 3 Na^+
406 out of the cell in exchange for only 2 K^+ , Na^+/K^+ -ATPase is the major driving force for the
407 excretion of H^+ *via* apical Na^+/H^+ -exchanger in acid excretory epithelial cells (Choe et al.,
408 2005; Edwards et al., 2002). As mentioned earlier, inhibiting both the Na^+/K^+ -ATPase and
409 basolateral K^+ -channels in brackish-water acclimated green crabs resulted in significantly
410 less ammonia excretion over the branchial epithelia (Weihrauch et al., 1998), a response
411 also seen in seawater-acclimated green crabs in this study. Even though to be treated with
412 caution as explained earlier, Siebers et al. (1994) identified Na^+/K^+ -ATPase to also be
413 involved in pH regulation in acid-base regulation. To the authors' knowledge this study is
414 the first to support these findings from osmo-regulating *C. maenas* also in osmo-
415 conforming, seawater-acclimated green crabs, strengthening the importance of Na^+/K^+ -
416 ATPase as a universal key-player in acid-base homeostasis.

417 While a likely electrogenic **Na⁺/H⁺-exchanger** (2Na⁺/H⁺) has been identified to be present
418 in crustacean gills (Shetlar and Towle, 1989), its localization is not clear to date. Inhibitor
419 experiments on isolated gills and spilt gill lamellae of osmo-conforming crabs like *Cancer*
420 *antenarius* and *Petrolishtes cinctipes* (Hunter and Kirschner, 1986) as well as *C. maenas*
421 (Weihrauch et al., 1998) indicated an apical distribution for this transporter, but follow-up
422 studies showed that effects of amiloride on ammonia excretion resulted from the inhibitor's
423 interference with the cuticle rather than directly targeting the epithelium (Onken and
424 Riestenpatt, 2002; Weihrauch et al., 2002). To the authors' knowledge, the present study
425 is the first to apply amiloride basolaterally in (seawater-acclimated) green crabs accounting
426 for *in-vivo* conditions. While Siebers et al. (1994) observed no differences in fluxes of acid-
427 base equivalents over the gill epithelium of brackish-water acclimated *C. maenas* when
428 Na⁺/H⁺-exchanger was inhibited by amiloride, these results have to be treated with caution
429 due to the composition of the perfusion solution. First of all, Siebers et al. (1994) applied
430 symmetrical conditions with diluted seawater as the bathing and perfusion solution that did
431 not contain any NH₄⁺. Additionally, the pH was buffered with TRIS basically eliminating
432 actual changes of free acid-base equivalents. However, a basolateral Na⁺/H⁺-exchanger has
433 been identified to be involved in acid-base regulation of gill epithelia in brackish-water
434 acclimated crabs *N. granulata* (Tresguerres et al., 2008), promoting intracellular Na⁺
435 uptake in exchange for H⁺ that is excreted into the hemolymph. A similar phenomenon has
436 also been observed in the TAL where NH₄⁺ has been shown to substitute for the H⁺ in
437 basolateral NHE4 to be transported into the blood in exchange for H⁺ (Bourgeois et al.,
438 2010; Weiner and Verlander, 2013). The most widely expressed isoform of Na⁺/H⁺-
439 exchanger to be found in virtually all vertebrate membranes, NHE1, has also been shown

440 to be present in the basolateral TAL and likely plays a more universal role as housekeeping
441 gene for pH and volume regulation (Bianchini et al., 1995; Landau et al., 2007). Supporting
442 an (additional) expression of Na^+/H^+ -exchanger in the cytoplasm are the findings of the
443 study by Nehrke and Melvin (2002) on the spoil-dwelling nematode *C. elegans*. In these
444 animals, NHX-3 is expressed in the vesicular membrane of the hypodermis, strengthening
445 the hypothesis of a vesicle-associated form of Na^+/H^+ -exchanger also in *C. maenas*.

446 The results for **carbonic anhydrase (CA)** in the present study have to be treated with
447 caution as the effects described are only obvious in the third perfusion step and not directly
448 in the inhibitor step. This is likely due to the inhibitor acetazolamide only slowly
449 penetrating the membranes therefore exhibiting its full effect only after a longer
450 application, respectively (Holder and Hayes, 1965; Teppema et al., 2001). As one of the
451 most ubiquitously expressed enzyme in all living organisms, carbonic anhydrase plays also
452 plays a crucial role in gills of decapod crustaceans by converting H^+ and HCO_3^- into CO_2
453 and H_2O , and vice versa (Henry & Cameron, 1983). In the gills of *C. maenas* two isoforms
454 of branchial carbonic anhydrase have been identified, a cytoplasmic and a membrane
455 bound isoform (Boettcher et al., 1990; Serrano and Henry, 2008). In teleost fish, mainly
456 the cytosolic isoform of carbonic anhydrase has been identified to be present in the gill
457 epithelium, while elasmobranchs gills express both cytosolic and membrane-bound
458 isoforms. Also in kidney both the cytosolic and membrane bound carbonic anhydrase play
459 a role in acid-base regulation (Gilmour and Perry, 2009). In osmo-conforming seawater-
460 acclimated green crabs, carbonic anhydrase activity is similar in all gills with a high
461 expression of the membrane-bound isoform, whereas upon acclimation to brackish-water
462 carbonic anhydrase activity increases 8-fold mainly due to an increase of the cytoplasmic

463 pool (Henry et al., 2003; Serrano and Henry, 2008). Data of the present study suggests the
464 involvement of both isoforms but indicates a potentially more important role for
465 membrane-bound carbonic anhydrase as the primary source for basolateral CO₂ entry into
466 the epithelial cell by generating ΔP_{CO_2} .

467

468 **Hypothesized mechanism for proton excretion over the anterior gill epithelium of**
469 **seawater-acclimated *C. maenas* (figure 5A)**

470 The major source for protons in the proposed model is the basolateral entry of CO₂ into the
471 epithelial cell, possibly through a basolateral Rhesus-like protein (Weihrauch, pers.
472 communication), and its immediate conversion to H⁺ and HCO₃⁻ by a membrane-bound
473 carbonic anhydrase (Serrano and Henry, 2008). Inhibiting (membrane-bound) carbonic
474 anhydrase ultimately results in less CO₂ to enter the cell and therefore also lower
475 intracellular H⁺ but higher hemolymph H⁺, translating into the observed decrease in H⁺
476 excretion rates. Taking into account the contribution of the cytoplasmic carbonic
477 anhydrase, less intracellular CO₂ would be present in the dissociated form, therefore again
478 lowering intracellular H⁺ concentrations and consequently its excretion as observed in the
479 present study.

480 As an additional proton source, NH₄⁺ can enter the epithelial cell *via* basolateral Na⁺/K⁺-
481 ATPase (supported by K⁺-channels; Skou, 1960) and dissociates to a certain degree into
482 H⁺ and NH₃ in the cytoplasm. Inhibiting basolateral Na⁺/K⁺-ATPase eliminates this direct
483 pathway, therefore providing less intracellular H⁺ and leading to its accumulation in the
484 hemolymph, therefore obviously resulting in the direct reduction of H⁺ excretion *via*
485 acidified vesicles. A similar effect is observed when basolateral K⁺-channels are inhibited:

486 the resulting build-up of intracellular K^+ will lead to a weakening of the electrochemical
487 gradient created by Na^+/K^+ -ATPase and the latter would not be able anymore to actively
488 transport NH_4^+/H^+ into the cell.

489 In the next step of the cascade, intracellular protons are pumped into vesicles mainly *via*
490 V-ATPase, possibly with the help of a vesicular Na^+/H^+ -exchanger. Within the vesicles,
491 H^+ traps NH_3 by forming NH_4^+ so that proton excretion *via* this suggested major H^+
492 excretory pathway is closely linked to ammonia excretion as hypothesized by (Weihrauch
493 et al., 1998). Targeting this hypothesized vesicular V-ATPase and Na^+/H^+ -exchanger with
494 the inhibitors KM91104 and amiloride, respectively, prevented H^+ from entering those
495 vesicles and consequently not being excreted *via* this pathway, explaining the observed
496 decrease in H^+ excretion. A basolateral Na^+/H^+ -exchanger on the other hand would provide
497 a way for H^+ out of the cell into the hemolymph and might help to regulate hemolymph
498 acid-base balance.

499 When the H^+ (NH_4^+) loaded vesicles containing V-ATPase reach the apical membrane,
500 they fuse and release their contents into the environment. This fusion is hypothesized to
501 provide the presence of an apical V-ATPase in the apical membrane which might promote
502 an additional, vesicular-independent way for proton excretion. This is supported by the
503 observed decrease of H^+ excretion as a result of apical application of KM91104 in the
504 present study. Additionally, this explains why the microtubule inhibitor colchicine alone
505 does not have a direct effect on H^+ excretion in the anterior gill epithelium of seawater-
506 acclimated green crabs as shown in the recent study by Fehsenfeld et al. (2015). When
507 basolateral Na^+/HCO_3^- -cotransporter is blocked, HCO_3^- accumulates in the hemolymph
508 while intracellular H^+ increases. This excess hemolymph HCO_3^- would need to be buffered

509 by H^+ , potentially provided by basolateral Na^+/H^+ -exchanger from the excess intracellular
510 pool of H^+ , therefore resulting in a decrease of H^+ excretion.

511

512 **Hypothesized mechanism for CO_2 excretion over the anterior gill epithelium of**
513 **seawater-acclimated *C. maenas* (figure 5B)**

514 Also in the hypothesized model for CO_2 excretion (figure 5B), the major pathway includes
515 a vesicular yet different transport mechanism, which is relatively independent from the
516 acidified vesicles proposed in figure 5A. As described earlier, CO_2 enters the cell over the
517 basolateral membrane by membrane diffusion or a recently described Rhesus-like protein
518 (Fehsenfeld et al. 2015; Weihrauch et al., 2004). The proposed immediate dissociation of
519 CO_2 to H^+ and HCO_3^- by carbonic anhydrase generates a ΔP_{CO_2} over the basolateral
520 membrane so that CO_2 fluxes are directed from the hemolymph into the epithelial cell. By
521 inhibiting this potential membrane-bound carbonic anhydrase and therefore the
522 dissociation of CO_2 into H^+ and HCO_3^- , the establishment of a ΔP_{CO_2} over the basolateral
523 membrane would be prevented, therefore leading to the accumulation of CO_2 in the
524 hemolymph instead (equal to a decrease in CO_2 excretion rates, as observed in the present
525 study). Additionally, a cytoplasmic carbonic anhydrase provides CO_2 from HCO_3^-
526 (entering by a basolateral Na^+/HCO_3^- -cotransporter) binding to excess intracellular H^+ ,
527 likely generated from the high protein metabolism of the gill (Weihrauch, 1998). When
528 blocked, less intracellular CO_2 is generated, also contributing to the observed decrease in
529 excretion rate.

530 As the next step in trans-branchial CO_2 excretion as hypothesized in the present study,
531 intracellular CO_2 is translocated into the hypothesized second class of not acidified vesicles

532 by Rhesus-like protein. Additionally, the Rhesus-like protein localized in the cytoplasm
533 and potentially associated with the vesicular membrane (Fehsenfeld et al., 2015) promotes
534 the entry of NH_3 into the vesicles. In the vesicle, CO_2 dissociates again into HCO_3^- and H^+
535 and the latter reacts with NH_3 to form NH_4^+ , therefore HCO_3^- and NH_4^+ are trapped in these
536 vesicles by carbonic anhydrase creating a concentration gradient over the vesicular
537 membrane for both ions. Support for this alternative vesicular pathway is coming from the
538 recent study of Fehsenfeld et al. (2015) as discussed above, where in the case of CO_2
539 blocking the microtubule network with colchicine was observed to result in a significant
540 decrease in CO_2 excretion. Inhibiting carbonic anhydrase can be postulated to decrease CO_2
541 excretion in a number of ways: first, by directly targeting basolateral membrane-bound
542 carbonic anhydrase and preventing its immediate dissociation into H^+ and HCO_3^- , ΔP_{CO_2}
543 over the basolateral membrane will be weakened and consequently lead to lower CO_2
544 influx into the cell and accumulation in the hemolymph. Secondly, similar effect can be
545 postulated for a potential vesicular isoform of carbonic anhydrase, resulting in less the
546 excretion of CO_2 -loaded vesicles. Finally, affecting the cytoplasmic pool of carbonic
547 anhydrase might lead to less generation of CO_2 from metabolically produced H^+ and
548 $\text{Na}^+/\text{HCO}_3^-$ -cotransporter -mediated HCO_3^- , therefore lowering intracellular CO_2 and
549 resulting in less vesicle-mediated CO_2 excretion.

550 The decrease of CO_2 excretion (translating into an increase in hemolymph CO_2) observed
551 when Na^+/K^+ -ATPase and K^+ -channels are blocked basolaterally can be attributed to the
552 indirect effect of the resulting accumulation of H^+ in the hemolymph as described above.
553 The excess hemolymph H^+ would be buffered by HCO_3^- by forming CO_2 , hence increasing
554 hemolymph $p\text{CO}_2$ and translating into a decrease of CO_2 excretion rates. HCO_3^- might

555 potentially be delivered by the basolateral $\text{Na}^+/\text{HCO}_3^-$ -cotransporter switching its direction
556 due to the change in concentration gradients for Na^+ over the basolateral membrane.
557 Finally, when basolateral $\text{Na}^+/\text{HCO}_3^-$ -cotransporter is blocked a major CO_2 -independent
558 intracellular source for HCO_3^- is eliminated and instead, HCO_3^- accumulates in the
559 hemolymph. This excess hemolymph HCO_3^- is buffered by H^+ (NH_4^+ ?) and creates CO_2 ,
560 resulting in the observed increase in hemolymph $p\text{CO}_2$ and translating in a net decrease of
561 CO_2 excretion over the epithelial membrane.

562

563 **Hypothesized mechanism for $\text{NH}_3/\text{NH}_4^+$ excretion over the anterior gill epithelium of**
564 **seawater-acclimated *C. maenas* (figure 5C)**

565 Generally, ammonia excretion as proposed in the hypothesized model of this study depends
566 to a significant amount on NH_3 trapping in both vesicular pathways as introduced in figure
567 5A and 5B. In contrast to H^+ and CO_2 excretion however, $\text{NH}_3/\text{NH}_4^+$ excretion does not
568 seem to depend on HCO_3^- entering the cell *via* basolateral $\text{Na}^+/\text{HCO}_3^-$ -cotransporter,
569 indicating that the transport in acidified vesicles and therefor the direct presence of H^+
570 might contribute to a bigger extend to this process than trapping NH_3 in CO_2 -enriched
571 vesicles.

572 As applying KM91104 basolaterally is believed to target the hypothesized vesicular V-
573 ATPase, the immediate result is the decrease in ammonia excretion *via* the proposed
574 acidified vesicles due to the lack of H^+ . Ammonia can still be excreted *via* the second CO_2 -
575 dependent vesicular pathway however, therefore excretion rates decrease by only 30%.
576 When inhibiting basolateral Na^+/K^+ -ATPase, a possible direct pathway for NH_4^+ (NH_3) to
577 enter the cell is decreased, resulting in the obvious direct reduction of $\text{NH}_3/\text{NH}_4^+$ excretion

578 *via* acidified vesicles. Again, a similar effect is observed when basolateral K^+ -channels are
579 inhibited due to the weakening of the electrochemical gradient created by Na^+/K^+ -ATPase,
580 so that the latter would not be able anymore to actively transport NH_4^+/H^+ into the cell.
581 Additionally, NH_4^+ might also substitute for the K^+ directly in the potentially bi-directional
582 channels and therefore an additional direct way for ammonia to possibly enter the cell
583 would be eliminated.

584 As discussed earlier, Na^+/H^+ -exchanger potentially directly promotes H^+ entry into
585 acidified vesicles. Therefore its inhibition is comparable to inhibition of V-ATPase and
586 would lead to the observed decrease of ammonia excretion *via* acidified vesicles.

587

588 **Acknowledgements**

589 The authors would like to thank Dr. Greg G. Goss, Dr. Chris M. Wood and Tamzin Blewett,
590 as well as the staff of the Bamfield Marine Sciences Center for the help in collecting the
591 green crabs and providing space and equipment. This work was funded by a NSERC
592 Discovery Grant (DW) and the University of Manitoba Graduate Fellowship (SF).

593

594 **Literature**

595 Appelhans, Y. S., Thomsen, J., Pansch, C., Melzner, F., & Wahl, M. (2012). Sour times:
596 Seawater acidification effects on growth, feeding behaviour and acid-base status of
597 *Asterias rubens* and *Carcinus maenas*. *Marine Ecology Progress Series*, 459, 85–97.

598 Bellwood, O. (2002). The occurrence, mechanics and significance of burying behaviour
599 in crabs (Crustacea: Brachyura). *Journal of Natural History*, 36, 1223–1238.

600 Bianchini, L., Kapus, A., Lukacs, G., Wasan, S., Wakabayashi, S., Pouysségur, J., ...
601 Grinstein, S. (1995). Responsiveness of mutants of NHE1 isoform of Na⁺/H⁺
602 antiport to osmotic stress. *The American Journal of Physiology*, 269(4), C998–
603 C1007.

604 Boettcher, K., Siebers, D., & Becker, W. (1990). Localization of carbonic anhydrase in
605 the gills of *Carcinus maenas*. *Comparative Biochemistry and Physiology Part B*,
606 96(2), 243–246.

607 Bourgeois, S., Van Meer, L., Wootla, B., Bloch-Faure, M., Chambrey, R., Shull, G. E.,
608 ... Houillier, P. (2010). NHE4 is critical for the renal handling of ammonia in
609 rodents. *Journal of Clinical Investigation*, 120(6), 1895–1904.
610 doi:10.1172/JCI36581

611 Brauner, C. J., & Baker, D. W. (2009). Patterns of Acid-base regulation during exposure
612 to hypercarbia in fishes. In M. L. Glass & S. C. Wood (Eds.), *Cardio-Respiratory*
613 *Control in Vertebrates* (pp. 263–284). Heidelberg: Springer-Verlag.

614 Burnett, L. E., Woodson, P. B., Rietow, M., & Vilicich, V. C. (1981). Crab gill intra-
615 epithelial carbonic anhydrase plays a major role in haemolymph CO₂ and chloride
616 ion regulation. *The Journal of Experimental Biology*, 92, 243–254.

- 617 Cameron, B., & Metaxas, A. (2005). Invasive green crab, *Carcinus maenas*, on the
618 Atlantic coast and in the Bras d'Or Lakes of Nova Scotia, Canada: larval supply and
619 recruitment. *Journal of the Marine Biological Association of the United Kingdom*,
620 85(4), 847–855.
- 621 Cameron, J. N. (1978). Effects of hypercapnia on blood acid-base status, NaCl fluxes,
622 and trans-gill potential in freshwater blue crabs, *Callinectes sapidus*. *Journal of*
623 *Comparative Physiology B*, 123(2), 137–141.
- 624 Choe, K. P., Kato, A., Hirose, S., Plata, C., Sindic, A., Romero, M. F., ... Evans, D. H.
625 (2005). NHE3 in an ancestral vertebrate: primary sequence, distribution,
626 localization, and function in gills. *American Journal of Physiology Regulatory*
627 *Integrative and Comparative Physiology*, 289(5), R1520–R1534.
- 628 Compere, P., Wanson, S., Pequeux, A., Gilles, R., & Goffinet, G. (1989). Ultrastructural
629 changes in the gill epithelium of the green crab *Carcinus maenas* in relation to the
630 external salinity. *Tissue & Cell*, 21(2), 299–318.
- 631 Ducoudret, O., Diakov, A., Müller-Berger, S., Romero, M. F., & Frömter, E. (2001). The
632 renal Na-HCO₃-cotransporter expressed in *Xenopus laevis* oocytes: Inhibition by
633 tenidap and benzamil and effect of temperature on transport rate and stoichiometry.
634 *Pflügers Archiv European Journal of Physiology*, 442(5), 709–717.
- 635 Edwards, S. L., Donald, J. a., Toop, T., Donowitz, M., & Tse, C. M. (2002).
636 Immunolocalisation of sodium/proton exchanger-like proteins in the gills of
637 elasmobranchs. *Comparative Biochemistry and Physiology Part A*, 131(2), 257–265.

- 638 Evans, D. H., Piermarini, P. M., & Choe, K. P. (2005). The multifunctional fish gill:
639 Dominant site of gas exchange, osmoregulation, acid-base regulation, and excretion
640 of nitrogenous waste. *Physiological Reviews*, 85, 97–177.
- 641 Fehsenfeld, S., Kiko, R., Appelhans, Y., Towle, D. W., Zimmer, M., & Melzner, F.
642 (2011). Effects of elevated seawater pCO₂ on gene expression patterns in the gills of
643 the green crab, *Carcinus maenas*. *BMC Genomics*, 12(1), 488.
- 644 Fehsenfeld, S., & Weihrauch, D. (2013). Differential acid-base regulation in various gills
645 of the green crab *Carcinus maenas*: Effects of elevated environmental pCO₂.
646 *Comparative Biochemistry and Physiology Part A*, 164, 54–65.
- 647 Freire, C., Onken, H., & McNamara, J. (2008). A structure-function analysis of ion
648 transport in crustacean gills and excretory organs. *Comparative Biochemistry and*
649 *Physiology, Part A*, 151(3), 272–304.
- 650 Gilmour, K., & Perry, S. (2009). Carbonic anhydrase and acid-base regulation in fish.
651 *The Journal of Experimental Biology*, 212, 1647–61.
- 652 Hammer, Ø., Harper, D. A. T., & Ryan, P. D. (2001). Past: Paleontological statistics
653 software package for education and data analysis. *Palaeontologia Electronica*, 4(1),
654 9–18.
- 655 Hans, S., Fehsenfeld, S., Treberg, J. R., & Weihrauch, D. (2014). Acid-base regulation in
656 the Dungeness crab (*Metacarcinus magister*). *Marine Biology*, 161(5), 1179–7793.

- 657 Hayashi, M., Kita, J., & Ishimatsu, A. (2004). Acid-base responses to lethal aquatic
658 hypercapnia in three marine fishes. *Marine Biology*, 144, 153–160.
- 659 Henry, R. P., & Cameron, J. N. (1982). Acid-base balance in *Callinectes sapidus* during
660 acclimation from high to low salinity. *Journal of Experimental Biology*, 101, 255–
661 264.
- 662 Henry, R. P., & Cameron, J. N. (1983). The role of carbonic anhydrase in respiration, ion
663 regulation and acid-base balance in the aquatic crab *Callinectes sapidus* and the
664 terrestrial crab *Gecarcinus lateralis*. *J. Exp. Biol.*, 103, 205–223.
- 665 Henry, R. P., Gehnrich, S., Weihrauch, D., & Towle, D. W. (2003). Salinity-mediated
666 carbonic anhydrase induction in the gills of the euryhaline green crab, *Carcinus*
667 *maenas*. *Comparative Biochemistry and Physiology, Part A*, 136(2), 243–258.
- 668 Henry, R. P., Lucu, Č., Onken, H., & Weihrauch, D. (2012). Multiple functions of the
669 crustacean gill: Osmotic/ionic regulation, acid-base balance, ammonia excretion, and
670 bioaccumulation of toxic metals. *Frontiers in Physiology*, 3, 1–33.
- 671 Holder, L. B., & Hayes, S. L. (1965). Diffusion of sulfonamides in aqueous buffers and
672 into red cells. *Molecular Pharmacology*, 1(3), 266–279.
- 673 Houillier, P., & Bourgeois, S. (2012). More actors in ammonia absorption by the thick
674 ascending limb. *American Journal of Renal Physiology*, 302, F293–F297.
675 doi:10.1152/ajprenal.00307.2011

676 Hu, M. Y., Guh, Y.-J., Stumpp, M., Lee, J.-R., Chen, R.-D., Sung, P.-H., ... Tseng, Y.-C.
677 (2014). Branchial NH_4^+ -dependent acid–base transport mechanisms and energy
678 metabolism of squid (*Sepioteuthis lessoniana*) affected by seawater acidification.
679 *Frontiers in Zoology*, 11, 55.

680 Hunter, K. C., & Kirschner, L. B. (1986). Sodium absorption coupled to ammonia
681 excretion in osmoconforming marine invertebrates. *The American Journal of*
682 *Physiology*, 251(5), R957–R962.

683 Jamieson, G. S., Grosholz, E. D., Armstrong, D. A., & Elner, R. W. (1998). Potential
684 ecological implications from the introduction of the European green crab, *Carcinus*
685 *maenas* (Linnaeus), to British Columbia, Canada, and Washington, USA. *Journal of*
686 *Natural History*, 32(10-11), 1587–1598.

687 Kartner, N., Yao, Y., Li, K., Crasto, G. J., Datti, A., & Manolson, M. F. (2010).
688 Inhibition of osteoclast bone resorption by disrupting vacuolar H^+ -ATPase $\alpha_3\text{-B}_2$
689 subunit interaction. *Journal of Biological Chemistry*, 285(48), 37476–37490.

690 Krapf, R. (1988). Basolateral membrane $\text{H}^+/\text{OH}^-/\text{HCO}_3^-$ transport in the rat cortical thick
691 ascending limb. *Journal of Clinical Investigations*, 82, 234–241.

692 Landau, M., Herz, K., Padan, E., & Ben-Tal, N. (2007). Model structure of the Na^+/H^+
693 exchanger 1 (NHE1): Functional and clinical implications. *Journal of Biological*
694 *Chemistry*, 282(52), 37854–37863.

695 Lignon, J. M. (1987). Ionic permeabilities of the isolated gill cuticle of the shore crab
696 *Carcinus maenas*. *The Journal of Experimental Biology*, 131, 159–174.

697 Lowe, S., Browne, M., Boudjelas, S., & De Poorter, M. (2000). *100 of the world 's worst*
698 *invasive alien species - A selection from the global invasive species database*
699 (2004th ed.). Auckland, New Zealand: ISSG/SSC/IUCN.

700 Lucu, Č., & Siebers, D. (1987). Linkage of Cl⁻ fluxes with ouabain sensitive Na/K
701 exchange through *Carcinus* gill epithelia. *Comparative Biochemistry and Physiology*
702 *Part A*, 87(3), 807–811.

703 Madhok, R. (1995). Tenidap. *Lancet*, 346, 481–485.

704 Martin, M., Fehsenfeld, S., Sourial, M. M., & Weihrauch, D. (2011). Effects of high
705 environmental ammonia on branchial ammonia excretion rates and tissue Rh-protein
706 mRNA expression levels in seawater acclimated Dungeness crab *Metacarcinus*
707 *magister*. *Comparative Biochemistry and Physiology, Part A*, 160(2), 267–77.

708 Miron, G., Audet, D., Landry, T., & Moriyasu, M. (2005). Predation potential of the
709 invasive green crab (*Carcinus maenas*) and other common predators on commercial
710 bivalve speices found on Prince Edward Island. *Journal of Shellfish Research*, 24(2),
711 579–586.

712 Nehrke, K., & Melvin, J. E. (2002). The NHX family of Na⁺-H⁺ exchangers in
713 *Caenorhabditis elegans*. *Journal of Biological Chemistry*, 277(32), 29036–29044.

- 714 Onken, H., & Putzenlechner, M. (1995). A V-ATPase drives active, electrogenic and
715 Na⁺-independent Cl⁻ absorption across the gills of *Eriocheir sinensis*. *The Journal of*
716 *Experimental Biology*, 198, 767–774.
- 717 Onken, H., & Riestenpatt, S. (2002). Ion transport across posterior gills of
718 hyperosmoregulating shore crabs (*Carcinus maenas*): amiloride blocks the cuticular
719 Na(+) conductance and induces current-noise. *The Journal of Experimental Biology*,
720 205, 523–531.
- 721 Onken, H., Tresguerres, M., & Luquet, C. M. (2003). Active NaCl absorption across
722 posterior gills of hyperosmoregulating *Chasmagnathus granulatus*. *The Journal of*
723 *Experimental Biology*, 206, 1017–1023.
- 724 Rao, K. P. (1958). Oxygen consumption as a function of size and salinity in *Metapenaeus*
725 *monoceros* Fab. from marine and brackish-water environments. *Journal of*
726 *Experimental Biology*, 35, 307–313.
- 727 Riestenpatt, S. (1995). *Die osmoregulatorische NaCl-Aufnahme über die Kiemen*
728 *decapoder Crustaceen (Crustacea, Decapoda)*. Berlin: VWF Verlag für
729 Wissenschaft und Forschung.
- 730 Riestenpatt, S., Onken, H., & Siebers, D. (1996). Active absorption of Na⁺ and Cl⁻ across
731 the gill epithelium of the shore crab *Carcinus maenas*: voltage-clamp and ion-flux
732 studies. *The Journal of Experimental Biology*, 199, 1545–54.

- 733 Serrano, L., & Henry, R. (2008). Differential expression and induction of two carbonic
734 anhydrase isoforms in the gills of the euryhaline green crab, *Carcinus maenas*, in
735 response to low salinity. *Comparative Biochemistry and Physiology Part D*, 3(2),
736 186–193.
- 737 Shetlar, R. E., & Towle, D. W. (1989). Electrogenic sodium-proton exchange in
738 membrane vesicles from crab (*Carcinus maenas*) gill. *The American Journal of*
739 *Physiology*, 257(4), R924–R931.
- 740 Siebers, D., Lucu, Č., Böttcher, K., & Jürss, K. (1994). Regulation of pH in the isolated
741 perfused gills of the shore crab *Carcinus maenas*. *Journal of Comparative*
742 *Physiology B*, 164(1), 16–22.
- 743 Siebers, D., Winkler, A., Lucu, C., Thedens, G., & Weichart, D. (1985). Na-K-ATPase
744 generates an active transport potential in the gills of the hyoerregulating shore crab
745 *Carcinus maenas*. *Marine Biology*, 87, 185–192.
- 746 Skou, J. C. (1960). Further investigations on a Mg^{++} + Na^{+} -activated
747 adenosinetriphosphatase, possible related to the active, linked transport of Na^{+} and
748 K^{+} across the nerve membrane. *Biochimica et Biophysica Acta*, 42, 6–23.
- 749 Stewart, P. A. (1978). Independent and dependent variables of acid-base control.
750 *Respiration Physiology*, 33, 9–26.

751 Teppema, L. J., Dahan, A., & Olievier, C. N. (2001). Low-dose acetazolamide reduces
752 CO₂-O₂ stimulus interaction within the peripheral chemoreceptors in the
753 anaesthetised cat. *Journal of Physiology*, 537(1), 221–229.

754 Thomsen, J., Gutowska, M., Saphörster, J., Heinemann, A., Trübenbach, K., Fietzke, J.,
755 ... Melzner, F. (2010). Calcifying invertebrates succeed in a naturally CO₂-rich
756 coastal habitat but are threatened by high levels of future acidification.
757 *Biogeosciences*, 7, 3879–3891.

758 Thomsen, J., & Melzner, F. (2010). Moderate seawater acidification does not elicit long-
759 term metabolic depression in the blue mussel *Mytilus edulis*. *Marine Biology*,
760 157(12), 2667–2676.

761 Towle, D., Henry, R., & Terwilliger, N. (2011). Microarray-detected changes in gene
762 expression in gills of green crabs (*Carcinus maenas*) upon dilution of environmental
763 salinity. *Comparative Biochemistry and Physiology Part D*, 6(2), 115–125.

764 Tresguerres, M., Parks, S., Sabatini, S., Goss, G. G., & Luquet, C. M. (2008). Regulation
765 of ion transport by pH and [HCO₃⁻] in isolated gills of the crab *Neohelice*
766 (*Chasmagnathus*) *granulata*. *American Journal of Physiology Regulatory Integrative*
767 *and Comparative Physiology*, 294(3), R1033–1043.

768 Truchot, J. (1976). Carbon dioxide combining properties of the blood of the shore crab
769 *Carcinus maenas* (L.): Carbon dioxide solubility coefficient and carbonic acid
770 dissociation constants. *The Journal of Experimental Biology*, 64, 45–57.

- 771 Truchot, J., & Duhamel-Jouve, A. (1980). Oxygen and carbon dioxide in the marine
772 intertidal environment: diurnal and tidal changes in rockpools. *Respirin Physiology*,
773 39, 241–254.
- 774 Truchot, J. P. (1981). The effect of water salinity and acid-base state on the blood acid-
775 base balance in the euryhaline cra, *Carcinus maenas* (L.). *Comparative Biochemistry*
776 *and Physiologie A*, 68, 555–561.
- 777 Weihrauch, D., Becker, W., Postel, U., Luck-Kopp, S., & Siebers, D. (1999). Potential of
778 active excretion of ammonia in three different haline species of crabs. *Journal of*
779 *Comparative Physiology B*, 169(1), 25–37.
- 780 Weihrauch, D., Becker, W., Postel, U., Riestenpatt, S., & Siebers, D. (1998). Active
781 excretion of ammonia across the gills of the shore crab *Carcinus maenas* and its
782 relation to osmoregulatory ion uptake. *Comparative Biochemistry and Physiologie*
783 *Part B*, 168, 364–376.
- 784 Weihrauch, D., McNamara, J. C., Towle, D. W., & Onken, H. (2004). Ion-motive
785 ATPases and active, transbranchial NaCl uptake in the red freshwater crab,
786 *Dilocarcinus pagei* (Decapoda, Trichodactylidae). *The Journal of Experimental*
787 *Biology*, 207, 4623–4631.
- 788 Weihrauch, D., Morris, S., & Towle, D. W. (2004). Ammonia excretion in aquatic and
789 terrestrial crabs. *The Journal of Experimental Biology*, 207, 4491–4504.

790 Weihrauch, D., Ziegler, A., Siebers, D., & Towle, D. W. (2001). Molecular
791 characterization of V-type H(+)-ATPase (B-subunit) in gills of euryhaline crabs and
792 its physiological role in osmoregulatory ion uptake. *The Journal of Experimental*
793 *Biology*, 204, 25–37.

794 Weihrauch, D., Ziegler, A., Siebers, D., & Towle, D. W. (2002). Active ammonia
795 excretion across the gills of the green shore crab *Carcinus maenas*: participation of
796 Na⁺/K⁺-ATPase, V-type H⁺-ATPase and functional microtubules. *The Journal of*
797 *Experimental Biology*, 205, 2765–2775.

798 Weiner, I. D., & Verlander, J. W. (2013). Renal ammonia metabolism and transport.
799 *Comprehensive Physiology*, 3, 201–220.

800 Zanders, I. P. (1980). Regulation of blood ions in *Carcinus maenas* (L.). *Comparative*
801 *Biochemistry and Physiology A*, 65, 97–108.

802

803

804 **Figures**

805 **Figure 1. Perfusion scheme for inhibitor experiments on isolated anterior gill 5 of**
806 **seawater-acclimated green crabs *Carcinus maenas*.** Gills were perfused with a perfusion
807 solution mimicking the ionic composition of hemolymph of seawater-acclimated (32 ppt)
808 green crabs. A control step of 40 min was performed before the inhibitor was applied for
809 subsequent 40 min, followed by a 40 min wash-out period to ensure that the gill was still
810 alive. All steps accounted for a 10 min equilibration period (dashed lines) after which the
811 perfusate was then collected for 30 min.

812

813 **Figure 2. Time series of changes in hemolymph acid-base parameters of seawater (32**
814 **ppt) acclimated *Carcinus maenas* during the first 48 hours of exposure to elevated**
815 **environmental $p\text{CO}_2$ (hypercapnia; 1% CO_2).** Changes in (A) hemolymph pH, (B)
816 hemolymph $p\text{CO}_2$, and (C) hemolymph HCO_3^- in high $p\text{CO}_2$ crabs (filled squares) versus
817 control crabs (filled diamonds). Hemolymph was drawn through a hole in the carapace
818 sealed with dental dam at 0, 6, 12, 24 and 48 hours. Asterisks denote significant differences
819 between control and high $p\text{CO}_2$ animals (student's t-test with $p < 0.05$).

820

821 **Figure 3. Excretion rates for ammonia and acid-base equivalents of isolated perfused**
822 **gills of seawater (35 ppt) and brackish-water (10 ppt) acclimated *Carcinus maenas*.**
823 Anterior gill 5 was perfused for 30 min with the respective perfusion solution mimicking
824 the ionic composition of their hemolymph. Loss of ammonia in the perfusate was measured
825 directly, whereas proton excretion was calculated from the change in perfusate pH. CO_2
826 excretion rates were calculated based on the measured pH and total carbon C_T as described

827 in material & methods. Asterisks denote significant differences between different gills of
828 the same salinity, whereas bars denote significant differences between the same gill of
829 different salinity acclimations (student's t-test with $p < 0.05$, $n = 4 - 7$).

830

831 **Figure 4. Relative changes in excretion rates for ammonia and acid-base equivalents**
832 **of isolated anterior gill 5 of seawater acclimated *Carcinus maenas* during gill**
833 **perfusion applying inhibitors.** (A) relative changes in ammonia excretion based on
834 ammonia loss in the perfusate, (B) relative changes in H^+ excretion based on pH changes
835 in the perfusate, and (C) relative changes in CO_2 excretion based on changes in pH and C_T
836 in the perfusate. B, basolateral; A, apical; NBC, Na^+/HCO_3^- -cotransporter; NKA, Na^+/K^+ -
837 ATPase; chan, channel; NHE, Na^+/H^+ -exchanger. Asterisks denote significant changes in
838 comparison to the excretion rate during control perfusion (bold dashed lines; paired t-test
839 with $p < 0.05$, $n = 4 - 8$). The light dashed lines indicate a 50% inhibition.

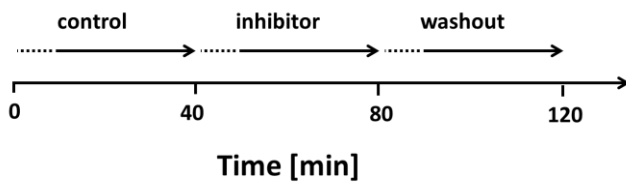
840

841 **Figure 5. Hypothetical model for acid-base regulation in the anterior gill epithelium**
842 **of seawater-acclimated *Carcinus maenas* and its link to ammonia excretion.** (A)
843 proposed mechanism for H^+ excretion, (B) proposed mechanism for CO_2 excretion, and
844 (C) proposed mechanism of NH_3/NH_4^+ excretion. Key-players have been identified in
845 perfusion experiments on isolated gill 5 applying inhibitory pharmaceuticals for the
846 respective components. Most drastic effects have been observed when blocking the V-
847 ATPase and Na^+/HCO_3^- -cotransporter basolaterally, leading to the postulation of two
848 different vesicle-dependent excretory pathways for ammonia and protons and ammonia

849 and CO₂. Details can be found in the text. Rh, Rhesus-like protein; CA, carbonic anhydrase;
850 ATP, ATPases (basolateral Na⁺/K⁺-ATPase, vesicular / apical V-ATPase).

851

852 **Figures**

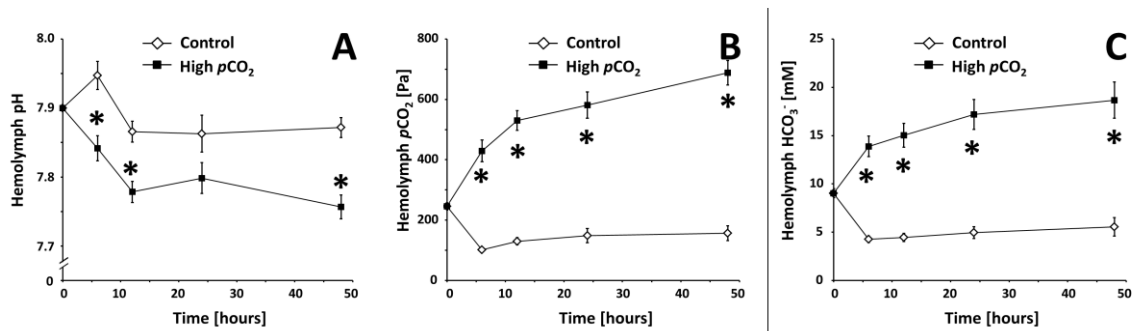


853

854 Figure 1.

855

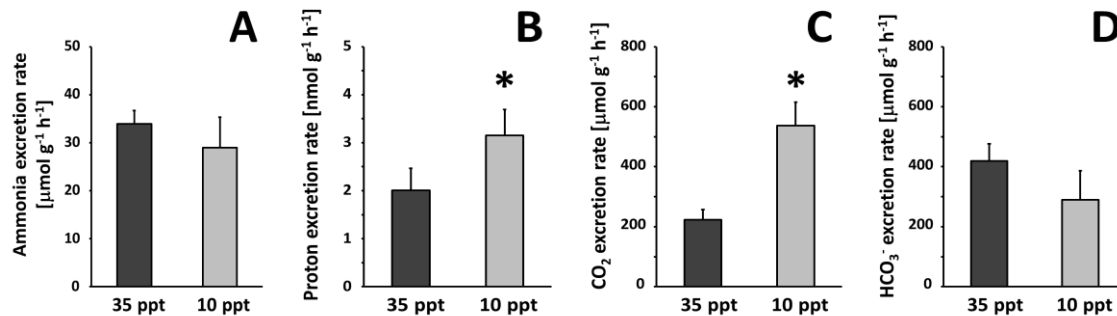
856



857

858 Figure 2.

859



860

861 Figure 3.

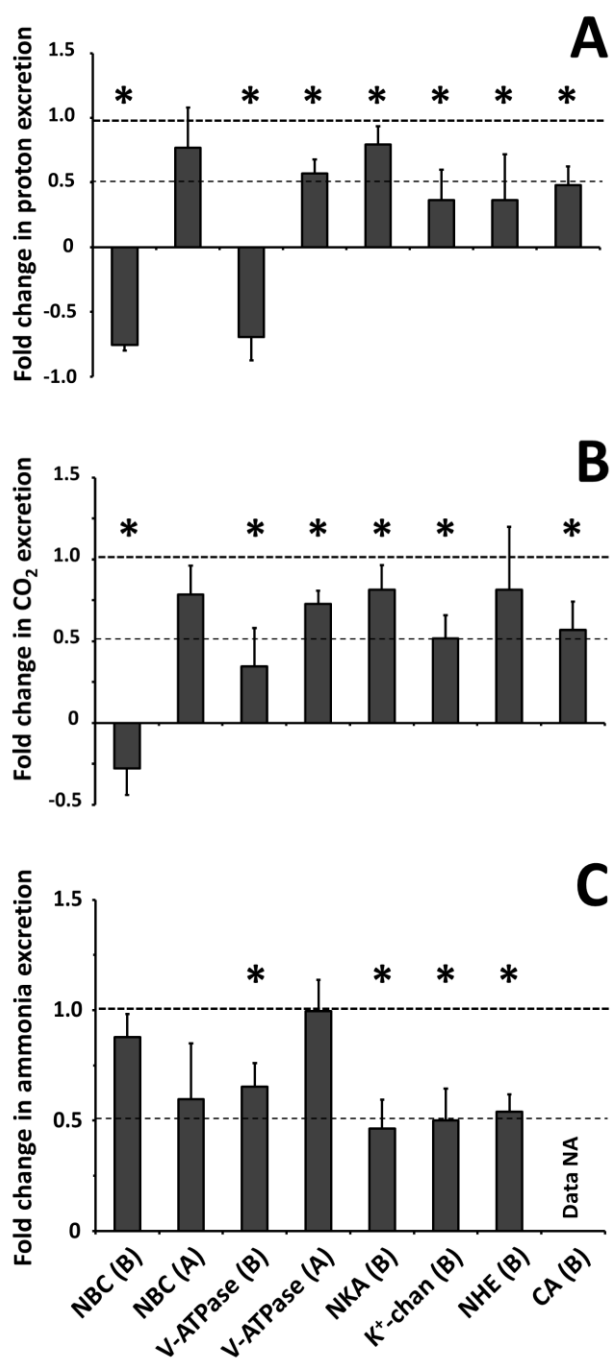
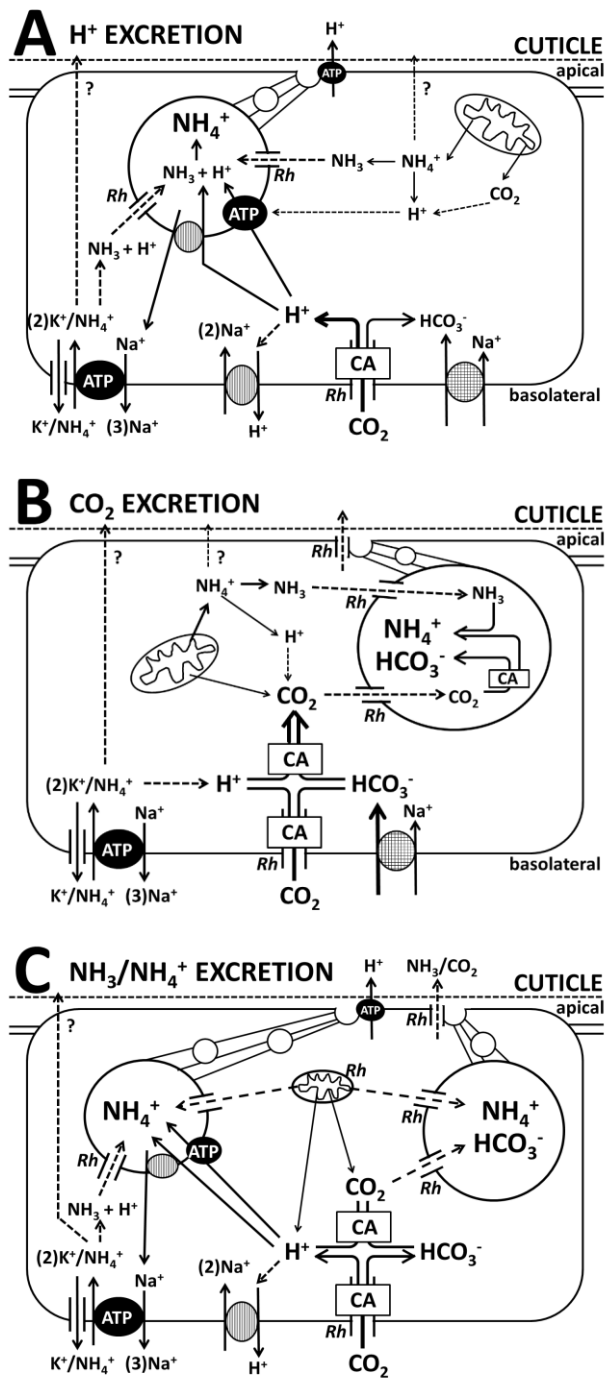


Figure 4.



868

869 Figure 5.